J. Physiol. (1984), **353**, *pp.* 585–608
With 11 *text-figures*
Printed in Great Britain

NON-SELECTIVE CONDUCTANCE IN CALCIUM CHANNELS OF FROG MUSCLE: CALCIUM SELECTIVITY IN A SINGLE-FILE PORE

BY W. ALMERS AND E. W. McCLESKEY

From the Department of Physiology and Biophysics, S.J.-40, University of Washington, Seattle, WA 98195, U.S.A.

(*Received 14 December 1983*)

SUMMARY

1. Voltage-clamp studies were carried out to compare currents through Ca^{2+} channels (I_{Ca}) with Na^+ currents (I_{ns}) through a non-selective cation conductance blocked by micromolar concentrations of external Ca^{2+}.

2. The gating of both currents was found to have similar time and voltage dependence. The amplitudes of I_{Ca} and I_{ns} varied widely, but I_{ns} was always large in fibres with large I_{Ca}, and small in fibres with small I_{Ca}. Both I_{Ca} and I_{ns} were blocked by the specific Ca^{2+} channel blocker nifedipine, with half-blockage concentrations that were virtually identical (K_D = 0·9 μM for I_{Ca} and 0·7 μM for I_{ns}). I_{Ca} and I_{ns} were also equally sensitive to block by diltiazem (K_D = 80 μM).

3. These parallels between I_{ns} and I_{Ca} are most easily explained if I_{ns} flows through Ca^{2+} channels. Apparently, Ca^{2+} channels bear high-affinity Ca^{2+}-binding sites, and are highly permeable to monovalent cations when Ca^{2+} is absent.

4. Ba^{2+} currents (I_{Ba}) and I_{Ca} were measured in external solutions containing mixtures of Ba^{2+} and Ca^{2+}. I_{Ba} is blocked by Ca^{2+}, as is I_{ns}. Adding Ba^{2+} to Ca^{2+} produces only small or no increases in current, as if Ba^{2+} is only sparingly permeant when Ca^{2+} is present. Membrane currents in Ba^{2+}/Ca^{2+} mixtures show anomalous mole-fraction behaviour, suggesting that Ca^{2+} channels are single-file, multi-ion pores.

5. Complex current transients are observed under maintained depolarizations in Na^+/Ca^{2+} and Ba^{2+}/Ca^{2+} mixtures. They suggest that in ion mixtures, Ca^{2+} channels transport Ca^{2+} in preference to Na^+ and Ba^{2+}. Hence Ca^{2+} channels are selective for Ca^{2+}, even though current amplitudes suggest that the Na^+ or Ba^{2+} permeabilities in the absence of Ca^{2+} are as high as, or higher than, the Ca^{2+} permeability.

6. We conclude that the selective permeability of Ca^{2+} channels depends on the presence of Ca^{2+}. In model calculations, our observations are explained as a consequence of Ca^{2+} channels being single-file pores. It is proposed that Ca^{2+} channels derive much of their ion selectivity from high-affinity Ca^{2+} binding sites located in an otherwise unselective aqueous pore.

INTRODUCTION

The preceding paper concerned a voltage-gated ion channel that is non-selectively permeable to alkali metal ions and blocked by external Ca^{2+} (Almers, McCleskey & Palade, 1984*a*). Block can be described approximately as requiring one Ca^{2+} binding to each channel with a dissociation constant $K_D = 0{\cdot}7\ \mu M$. With a physiological external [Ca^{2+}] of 2 mM, it is difficult to see how this non-selective conductance could persist *in vivo*. Therefore one asks whether this seemingly new ion channel may, in fact, be one of the known channels operating in an abnormal mode. Here we demonstrate that the non-selective conductance mechanism and the Ca^{2+} channel share many common features, and propose that the two are identical. Evidently, the physiologically important ability of Ca^{2+} channels to exclude Na^+ and K^+ (e.g. Reuter & Scholz, 1977; Almers *et al.* 1984*a*) depends specifically on the presence of Ca^{2+}. This work has been communicated in abstract form (Almers, McCleskey & Palade, 1982) and similar conclusions were also reached in parallel work on snail neurones (Kostyuk, Mironov & Shuba, 1983).

Ca^{2+} channels are well known to be highly permeable to Ba^{2+}. We find that Ca^{2+} greatly diminishes the Ba^{2+} permeability of Ca^{2+} channels, as was previously observed in cardiac muscle (Hess, Lee & Tsien, 1983). Evidently Ca^{2+} enables the channel to reject not only Na^+ but also Ba^{2+}. One way to explain such an extreme dependence of ion permeability on the presence of the physiological substrate is to view the Ca^{2+} channel as an aqueous pore containing two or more binding sites along which the permeant ions must move in single file. Indeed Ca^{2+} channels in Ca^{2+}/Ba^{2+} mixtures show 'anomalous mole-fraction behaviour' (see also Hess *et al.* 1983), an effect considered characteristic for single-file pores (Hille & Schwarz, 1978). In model calculations, we explore the behaviour of Ca^{2+} channels in solutions containing both Na^+ and Ca^{2+}, or Ba^{2+} and Ca^{2+}. It is shown that, with the appropriate rate constants, the observed Ca^{2+}-dependent changes in permeability are predicted if Ca^{2+} channels are single-file pores.

METHODS

Dissection and recording

Pieces of single fibres were dissected from the semitendinosus muscle of *Rana temporaria* and then voltage clamped with the vaseline-gap technique (Hille & Campbell, 1976), as described previously (Almers *et al.* 1984*a*). The length of fibre under voltage clamp varied from 0·3 to 0·5 mm and is given as the 'gap' width in Figure legends. It was continuously superfused with saline. Fresh fibres were used throughout. Before experiments started, a period of 20–30 min was allowed after the final cutting of fibre ends in one of the internal solutions (see below). This allowed the internal solution to enter the myoplasm by diffusion.

Throughout, membrane currents were corrected for capacitive and leakage currents by a combination of analog and digital techniques. They were filtered by a four-pole low-pass Bessel filter with a corner frequency of 100 Hz for 4 s depolarizations, and to 200 or 400 Hz for shorter pulses. Temperature was 20–25 °C.

Solutions

The composition of external solutions is given in Table 1, and the source of chemicals is given in the preceding paper (Almers *et al.* 1984*a*). Throughout, the methylsulphonate salts of Ca^{2+} were prepared by titrating $CaCO_3$ with methylsulphonic acid.

The end-pool, or internal, solutions bathed the cut fibre ends. They all contained 5 mM-morpholinopropanesulphonic acid (MOPS) titrated to pH 7 with tetramethylammonium (TMA^+)

hydroxide. Other constituents were as follows: Solution A, 80 mM-$(TMA)_2$EGTA; Solution B, 80 mM-$(TEA)_2$EGTA; Solution C, 20 mM-$(TMA)_2$EGTA plus 58 mM-TMA aspartate plus 32 mM-Cs aspartate; Solution D, 58·4 mM-$(TMA)_2$EGTA plus 32 mM-Cs aspartate; Solution E, 40 mM-$(TMA)_2$EGTA and 60 mM-TMA aspartate. Sometimes 5 mM-Mg aspartate was added to Solutions A, B, D or E (see Figure legends). Using published stability constants, the concentration of free Mg^{2+} is calculated as being 1·4 mM for Solutions A and B, 1·7 mM for Solution D and 2·9 mM for Solution E.

Nifedipine was obtained as a gift from Pfizer Pharmaceutical Company (New York, NY). A 2 mM-nifedipine solution in ethanol was prepared as a stock and stored at −20 °C in a light-tight container. Diltiazem was obtained as a gift from Marion Laboratories Inc. (Kansas City, MO). A 20 mM-diltiazem solution in water was prepared as a stock and stored frozen.

TABLE 1. External solutions

Solution	$Ca(MeSO_3)_2$	$BaCl_2$	TMA $MeSO_3$	Na $MeSO_3$
1	10	—	108	—
2	—	10	108	—
3	20	—	102·4	—
4	10	10	102·4	—
5	10	—	83·2	32
6	See legend			

All concentrations in mM. Solutions 1–5 contained, in addition, 1 μM-tetrodotoxin, 10 mM-MOPS (morpholinopropanesulphonic acid) and about 5 mM-tetramethylammonium (TMA^+) hydroxide to adjust pH to 7·0. Solution 6 was identical to Solution 9 of Almers *et al.* (1984*a*) and contained 10 mM-$CaSO_4$, 32 mM-NaOH, 130 mM-TMAOH, 32 mM-NaOH, 66 mM-EGTA and 22 mM-MOPS. Its pCa is calculated as 7·2, its pH was 7·0.

RESULTS

Similarities between non-selective conductance and Ca^{2+} channel

Fig. 1 shows membrane currents during step depolarizations from −100 mV to various potentials. 30 min before the beginning of the experiment, the fibre ends had been cut in a solution containing 32 mM-Cs^+ and the large and presumably impermeant TMA^+ as the main cations, and we expect that much of the myoplasmic K^+ had left the fibre. For the right-hand column of traces, the external solution contained TMA^+ and 10 mM-Ca^{2+} as the only cations. Inward currents are seen to rise slowly to a peak and decline thereafter. They remain inward even at the most positive potentials explored. As in previous work (Almers & Palade, 1981) we believe these currents to be essentially pure Ca^{2+} current (I_{Ca}).

On the left of Fig. 1, the external solution contained TMA^+ and 32 mM-Na^+ but essentially no Ca^{2+} (pCa = 7·2). Under these conditions, one records currents that reverse direction at about 0 mV and are blocked by micromolar concentrations of external Ca^{2+}. The inward current is carried by Na^+ since it vanishes when this ion is replaced by TMA^+, while the outward current is presumably carried by Cs^+ as well as residual K^+ in the myoplasm. Since this current flows through a non-selective conductance pathway (Almers *et al.* 1984*a*), we call it I_{ns}.

In Fig. 2, the currents in Fig. 1 are plotted against potential, each trace being evaluated at the time when current amplitude is largest. Besides reversing at ~ 0 mV, I_{ns} also turns on at ~ 30 mV more negative potentials than does I_{Ca}. That I_{ns} is activated at such negative potentials may be related to withdrawal of external Ca^{2+},

which in many experimental systems makes the external surface potential of the cell membrane more negative. To allow for this in Fig. 1, we have put traces next to each other that were recorded at potentials differing by 30 mV.

Fig. 1 shows that non-selective and Ca^{2+} channels respond similarly to changes in membrane potential. Both channels open with similar speed upon depolarization,

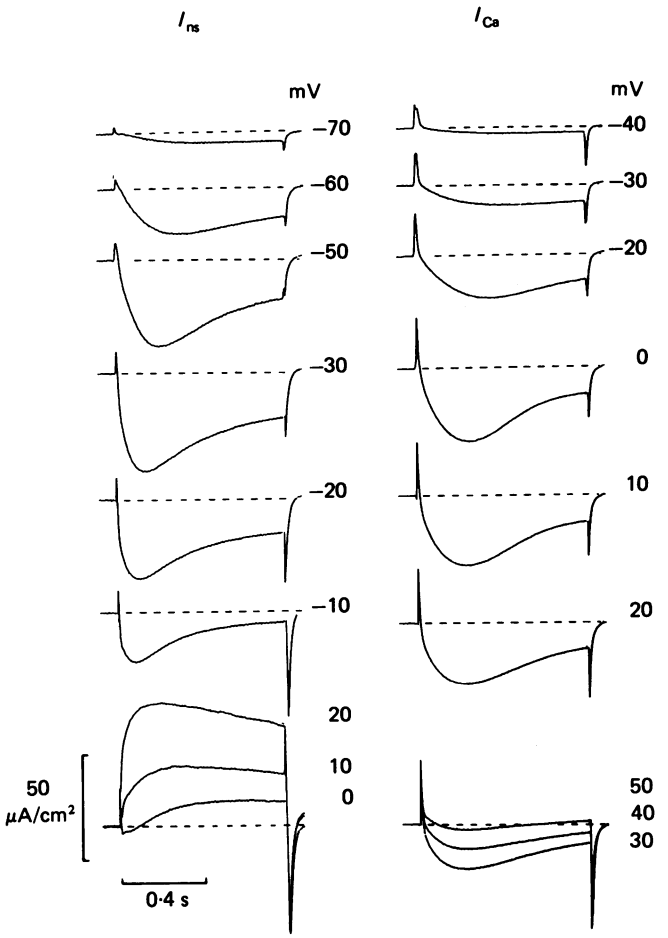

Fig. 1. Membrane currents during potential steps to the potentials indicated. The external solution contained first 32 mM-Na^+ and essentially no free Ca^{2+} (pCa = 7·2, Solution 6, left-hand traces, I_{ns}) and then no Na^+ but 10 mM-Ca^{2+} (Solution 1, I_{Ca}). Holding potential −100 mV, ends cut in Solution A with 5 mM-Mg aspartate added. Fibre no. 3035, diameter 145 μm, gap 350 μm.

with inward current reaching half its peak value in 38 ± 15 ms (I_{ns} at −20 mV) and 70 ± 14 ms (I_{Ca} at 10 mV; $n = 5$, ± standard deviation throughout). Both I_{ns} and I_{Ca} decline slowly if depolarization is maintained. With I_{Ca} this is due to Ca^{2+} depletion from the transverse tubules, and the same may be true for I_{ns}. Finally, both channels shut rapidly on repolarization. Judged by the decline of inward current tails at −100 mV after step depolarizations to −20 mV and 10 mV, non-selective and Ca^{2+}

channels close with time constants of 8·2 ± 1·8 ms (I_{ns}) and 10·6 ± 3·6 ms (I_{Ca}, $n = 10$, ± S.D.). The comparison shows that in kinetics and voltage dependence the non-selective conductance mechanism resembles the Ca^{2+} channel more than any other voltage-dependent cation channel known in skeletal muscle. If the non-selective conductance is due to one of the already known ion channels operating in an abnormal mode, it is probably due to the Ca^{2+} channel.

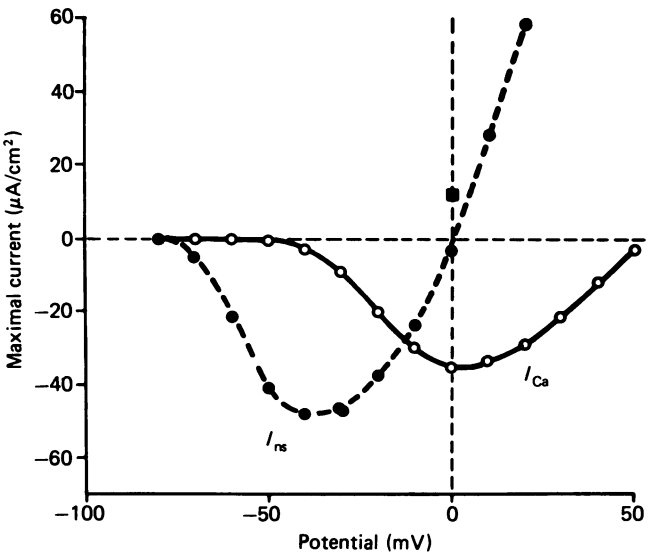

Fig. 2. Maximal currents in Fig. 1 plotted against potential. The square at 0 mV represents the final outward current and the dot the peak inward current, both obtained at 0 mV and in Solution 6.

In the following experiments, we will compare various aspects of I_{Ca} and I_{ns}. Throughout, these currents will be recorded as in Fig. 1. I_{Ca} will be recorded with 10 mM-Ca^{2+}, and I_{ns} with 32 mM-Na^{+}, as the only external permeant cation. When recording I_{ns}, external [Ca^{2+}] will always be buffered to pCa = 7·2 with a Ca^{2+}–EGTA mixture (see Methods).

Amplitudes of I_{Ca} and I_{ns} are correlated

The amplitude of I_{ns} was highly variable. Fig. 3*A* and *C* shows traces of I_{ns} from two different fibres. Though the traces were recorded under identical conditions, their amplitudes differed 8-fold. This difference is not primarily related to differences in fibre diameter, since the fibre diameters in Fig. 3*A* and *C* were not very different. More likely, the observed variability reflects a highly variable density of ion channels carrying I_{ns}.

The amplitude of I_{Ca} is similarly variable (see also Almers, Fink & Palade, 1981), and Fig. 3*B* and *D* shows I_{Ca} recorded from the pair of fibres in Fig. 3*A* and *C*. Apparently the fibre with small I_{ns} also had a small I_{Ca}, and the fibre with a large I_{ns} had a large I_{Ca}. Fig. 3*E* summarizes results from many similar experiments, plotting peak I_{ns} against peak I_{Ca}. Each point originates from a different fibre and

represents a pair of records as in Figs. 3*A* and *B* or 3*C* and *D*. In order to correct for differences in tubule membrane area related to different fibre diameters (Hodgkin & Nakajima, 1972), currents were referred to fibre volume. Throughout, the amplitudes of I_{ns} and I_{Ca} were found to be linearly correlated, with a correlation coefficient of $r = 0{\cdot}96$. Fig. 3 indicates that the molecular units responsible for I_{ns} and I_{Ca} are either identical or occur in the membrane at fixed stoicheiometry.

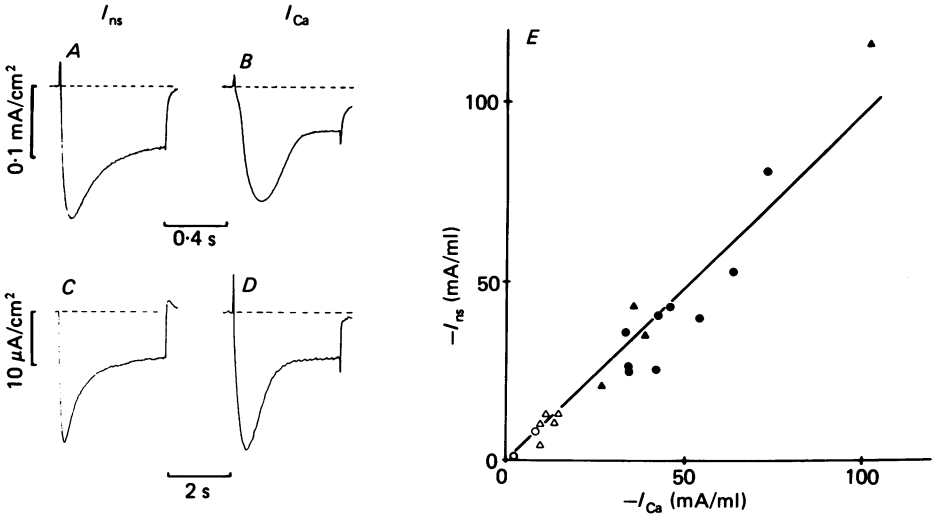

Fig. 3. *A–D*, I_{ns} and I_{Ca} recorded during potential steps to −20 mV (*A* and *C*) or 0 mV (*B* and *D*) and in the external solutions used in Fig. 1. Traces in *A* and *B*, from fibre no. 1902 with diameter 90 μm, gap 280 μm and ends cut in Solution E. *C* and *D*: from fibre no. 3061 with diameter 120 μm, gap 500 μm and ends cut in a solution similar to E but containing TEA^+ in place of TMA^+ and with 5 mM-Mg aspartate added. Holding potential −100 mV throughout. *E*, peak I_{ns} plotted against peak I_{Ca} in experiments as in *A–D*. Each point is from a different fibre. Throughout, I_{ns} at −20 mV was recorded first, and I_{Ca} at 0 mV, 3–44 min later. Experimental conditions varied as follows. Circles: ends cut in Solutions A, B, or E containing, in two cases, TEA^+ in place of TMA^+; triangles: ends cut in Solutions D or E; filled symbols: measurements made in summer 1982; open symbols: measurements made in winter 1983 and with 5 mM-Mg aspartate added to the solutions bathing the fibre ends. Using published stability constants, the free $[Mg^{2+}]$ of the solution is calculated as 1·4 (Solutions A and B) or 2·9 mM (Solution E).

Comparison of Figs. 3*B* and *D* shows that the larger I_{Ca} also declined more rapidly. This is generally observed under our experimental conditions, because the decline is due to Ca^{2+} depletion from the transverse tubular system. Comparison of Figs. 3*A* and *C* suggests that I_{ns} behaves similarly, as if Na^+ depletion from the tubules contributed to the decline. Though this possibility was not investigated in detail, Na^+ depletion would be expected since I_{ns} flows across the membrane of the transverse tubules (Takeda, 1977; Potreau & Raymond, 1982), as does I_{Ca}.

Block by drugs

The dihydropyridines nifedipine and nitrendipine are widely regarded as specific blockers of Ca^{2+} channels, and nitrendipine is now being used as a specific ligand to Ca^{2+} channels (for skeletal muscle transverse tubules, see Fosset, Jaimovitch,

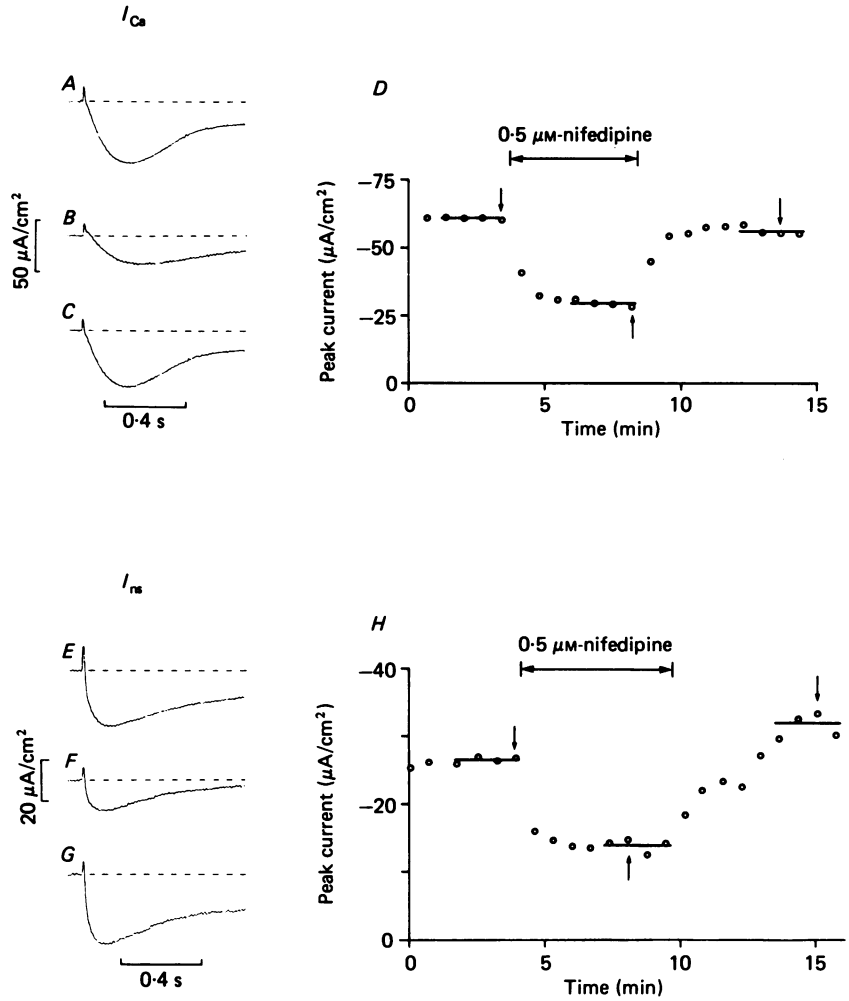

Fig. 4. Left: currents during depolarizations to +20 mV (*A–C*) or −30 mV (*E–G*) without drug (*A* and *E*), with 0·5 μM-external nifedipine (*B* and *F*) and after wash-out of the drug (*C* and *G*). Right: peak current at 20 mV (*D*) or −30 mV (*H*) as a function of time. In each graph, the three points marked by arrows were obtained from the traces on the left. Horizontal lines indicate an average calculated from the last four traces before a solution change. *A–D* from fibre no. 2502, diameter 90 μm, gap 240 μm. External Solution 1, ends cut in Solution E, holding potential −80 mV. *E–H* from fibre no. 3034, diameter 80 μm, gap 300 μm. External Solution 6, ends cut in Solution D with 5 mM-Mg^{2+} aspartate added (free [Mg^{2+}] 1·7 mM). Holding potential −100 mV throughout.

Delpont & Lazdunski, 1983). Fig. 4 shows that nifedipine reversibly blocks both I_{Ca} and I_{ns} to similar degrees. Peak values of I_{Ca} and I_{ns} are plotted against time while nifedipine is added and withdrawn. The horizontal lines indicate our estimates of the steady-state levels of current, both with drug and without. Dividing currents in the presence of drug by the average of currents before and after, one finds that at 0·5 μM-nifedipine, currents remaining were about 50% for both I_{Ca} and I_{ns}.

Fig. 5 is a dose–response curve summarizing experiments similar to that of Fig. 4. Points with error bars are averages of three to six determinations, points without

error bars are single measurements. To within experimental error, the points for I_{Ca} (dots) are described by one drug molecule blocking one Ca^{2+} channel, with a dissociation constant of $K_D = 0{\cdot}9 \pm 0{\cdot}09$ μM (S.D.) (least-squares fit, continuous line). For I_{ns} (circles) the best least-squares fit of the same model requires a value ($K_D = 0{\cdot}7 \pm 0{\cdot}09$ μM) that is identical within experimental error. Evidently I_{ns} and

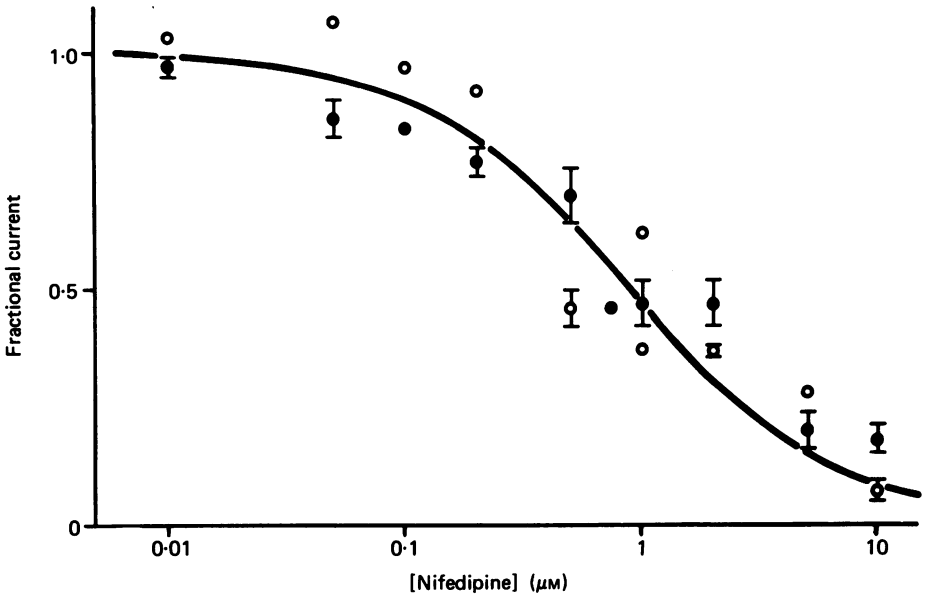

Fig. 5. Peak I_{ns} (circles) and I_{Ca} (dots) as a function of nifedipine concentration. All data from experiments as in Fig. 4. Fractional current was calculated by dividing currents in the presence of drug by the average of currents measured before drug application and after wash-out. Points with error bars (±S.E. of mean) are the mean of three to five measurements; points without error bars are single measurements. The continuous curve is given by $K_D/(K_D + [\text{nifedipine}])$ with $K_D = 0{\cdot}9 \pm 0{\cdot}09$ μM (S.D.) providing the best least-squares fit to the I_{Ca} data. The best estimate of K_D for the I_{ns} data was $0{\cdot}7 \pm 0{\cdot}09$ μM.

I_{Ca} are about equally sensitive to nifedipine. The values obtained here may be compared with that reported by Lee & Tsien (1983) for block of cardiac Ca^{2+} channels by nitrendipine (0·15 μM).

We also investigated the Ca^{2+} channel blocker diltiazem. In resting or infrequently stimulated cardiac muscle, the diltiazem concentration for 50% block of I_{Ca} is somewhat less than 5 μM (Lee & Tsien, 1983). In experiments similar to that in Fig. 4*A–D*, we found this drug to be much less effective in skeletal muscle, with a half-blockage concentration $K_D = 80 \pm 14$ μM (±S.D., eight fibres). Fig. 6 compares drug effects on I_{ns} and I_{Ca}. First, I_{ns} was recorded; 100 μM-diltiazem reduced peak current amplitude to about 40% of control. The external solution was then changed to one appropriate for measuring I_{Ca}. After drug removal, I_{Ca} increased within a few minutes to an approximately 2-fold larger steady value, indicating about 50% block. Once again, I_{ns} and I_{Ca} are blocked about equally.

Ca^{2+} as a blocker of Ca^{2+} channels

The above similarities between I_{ns} and I_{Ca} strongly suggest that both pass through the same ionic channel. If so, the blockage of I_{ns} by external Ca^{2+} implies that Ca^{2+} blocks Ca^{2+} channels. This seems in conflict with the finding that, as expected for a permeant ion, increasing external Ca^{2+} ($[Ca^{2+}]_o$) increases I_{Ca} rather than diminishing

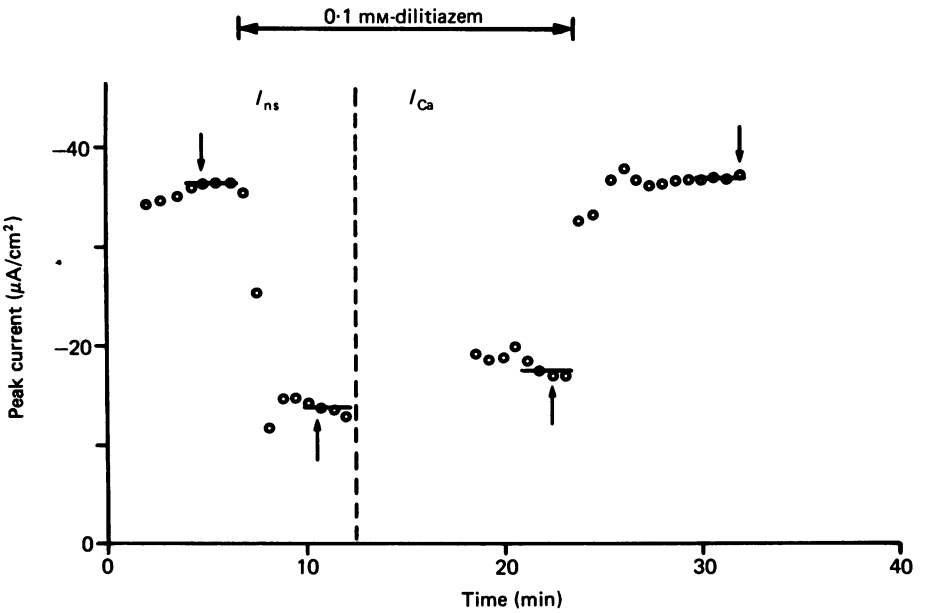

Fig. 6. Diltiazem block of I_{ns} and I_{Ca}. First, I_{ns} is measured in Solution 6 and then I_{Ca} is measured in Solution 1. 0·1 mM-diltiazem is present at the times indicated. The horizontal lines represent the average of the last four measurements before solution changes, and indicate our estimates of the steady states. Holding potential −100 mV, ends cut in Solution D with 5 mM-Mg aspartate added. Fibre no. 3052, diameter 160 μm, gap 390 μm.

it (see, for example, Fig. 11). In cardiac muscle, however, Ca^{2+} is readily shown to block Ba^{2+} currents (I_{Ba}) through Ca^{2+} channels (Hess *et al.* 1983), and similar results were obtained here. Fig. 7 shows currents in Na^+-free solutions containing 10 mM-Ba^{2+} (left) and 10 mM-Ca^{2+} (right), either singly (light traces) or with another divalent ion added, as indicated (heavy traces). Comparison of the light traces in Fig. 7 *A* and *B* (see also Figs. 8 and 9) shows that peak I_{Ba} is larger than I_{Ca}; as in other tissues (e.g. Hagiwara & Ohmori, 1982), Ba^{2+} is evidently more permeant than Ca^{2+}. The heavy trace in Fig. 7 shows that current in 10 mM-Ba^{2+} is strongly reduced by 1 mM-Ca^{2+}. A quantitative comparison is difficult because, with both $[Ca^{2+}]$ and $[Ba^{2+}]$ in the tubules diminishing due to depletion (Almers *et al.* 1981) the size and time course of currents are influenced in complicated ways (see later). The simplest assumption one can make is that adding 1 mM-Ca^{2+} to 10 mM-Ba^{2+} does not change the gating of Ca^{2+} channels. Then one may compare currents at early times where depletion will be less. If readings are taken 100 ms after depolarization when I_{Ba} (light trace) is at its peak,

one finds that 1 mM-Ca^{2+} reduced current to 33 % (43 % in another, similar experiment). I_{Ba} must have been reduced even more since Ca^{2+} will have contributed to inward current, probably more than in proportion to its concentration (see later). Hence the Ca^{2+} concentration that halves I_{Ba} is considerably less than 1 mM.

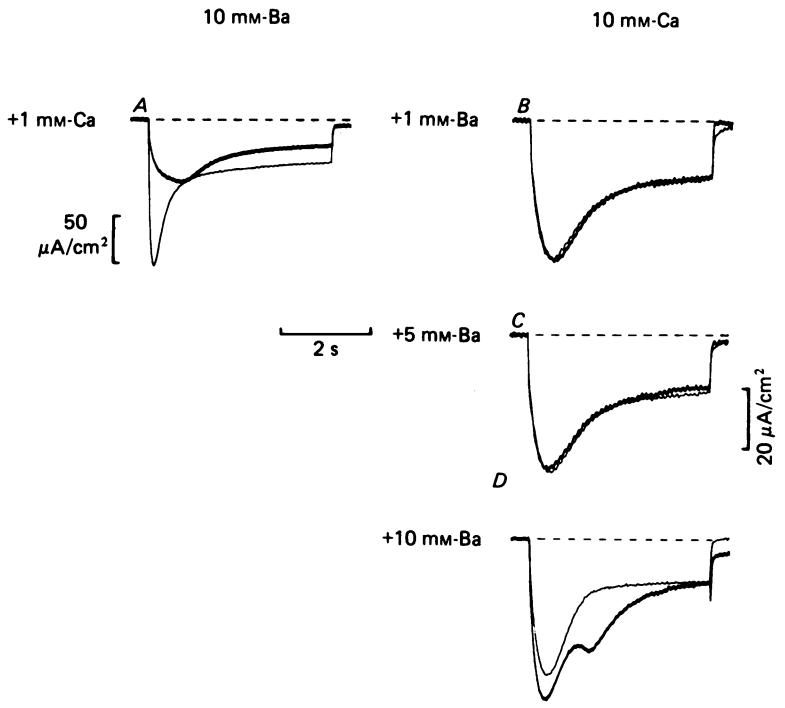

Fig. 7. Interaction of Ba^{2+} and Ca^{2+} in Ca^{2+} channels. The Figure shows membrane currents during step depolarizations to −10 mV (*A* and *D*) or +10 mV (*B* and *C*) from a holding potential of −80 mV. Throughout, light traces were recorded in a solution containing only Ca^{2+} (Solution 1) or only Ba^{2+} (Solution 2) as divalent cations; heavy traces were recorded in solutions containing both Ba^{2+} and Ca^{2+}. Concentrations of Ba^{2+} and Ca^{2+} are given in mM next to each trace. Ca^{2+} was added to Solution 2 as the methylsulphonate salt; Ba^{2+} was added to Solution 1 as $BaCl_2$. *A*, fibre no. 3071, diameter 80 μm, gap 250 μm; *B* and *C*, fibre no. 3073, diameter 90 μm, gap 250 μm; *D*, fibre no. 3070, diameter 120 μm, gap 300 μm. Ends cut in Solution B with 5 mM-Mg aspartate added.

Figs. 7*B*, *C* and *D* show the converse experiment where varying amounts of Ba^{2+} are added to 10 mM-Ca^{2+}. With 1 mM- and 5 mM-Ba^{2+}, no significant changes in current are evident. Only with 10 mM-Ba^{2+} did we consistently observe an increase in peak current, but the change was small. Fig. 7 suggests that Ba^{2+}, though highly permeant when Ca^{2+} is absent, is only sparingly permeant when Ca^{2+} is present. Thus Ca^{2+} affects I_{Ba} and I_{ns} similarly.

Anomalous mole-fraction behaviour

While adding Ba^{2+} to Ca^{2+} never caused a convincing decline of peak current in our experiments, there is nevertheless clear evidence of interaction between Ba^{2+} and Ca^{2+} in Ca^{2+} channels. In Fig. 8 (left), all current traces were recorded at −10 mV.

The divalent cations Ba^{2+} and Ca^{2+} were present either singly or as a mixture, but always at a total concentration of 10 mM. With 10 mM-Ba^{2+}, peak current is twice as large as with 10 mM-Ca^{2+}, but when both ions are present in a 1:1 mixture the current is smaller than when the less permeant ion is present singly. Other similar

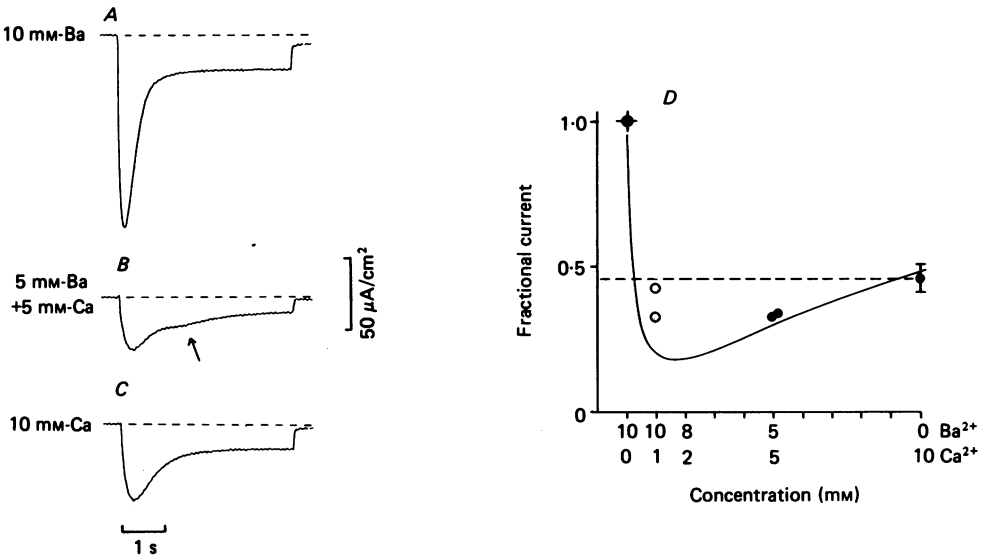

Fig. 8. *A–C*, membrane currents during step depolarizations from −80 mV to −10 mV in 10 mM-Ba^{2+} (Solution 2), then in a 1:1 mixture of Solutions 1 and 2 (5 mM-Ba^{2+} + 5 mM-Ca^{2+}) and then in 10 mM-Ca^{2+} (Solution 1). Ends cut in Solution B with 5 mM-Mg aspartate added. Fibre no. 3066, diameter 150 μm, gap 320 μm. *D*, fractional peak currents in solutions containing Ca^{2+} and Ba^{2+} in various proportions. Circles were obtained as in Fig. 7*A* (for analysis see text), that is, in Solution 2 with 1 mM-$Ca(CH_3SO_3)_2$ added. The *continuous curve* is predicted by a model described in the Discussion. Ba^{2+} and Ca^{2+} were assumed to interact identically with Ca^{2+} channels except for Ba^{2+} having slightly lower entrance barriers (9·15 *RT* each instead of 10·3 *RT* in Fig. 10) and, consistent with experimental results on snail neurones (Kostyuk *et al.* 1983), a 70-fold lower affinity for the binding sites associated with Ca^{2+} channels (energy wells: −10·3 *RT* each). The central energy barriers were the same for Ca^{2+} and Ba^{2+}. Any effects or contributions of other cations present intra- and extracellularly (TMA^+) were neglected.

experiments are summarized on the right of Fig. 8. The horizontal line (dashed) indicates the average fractional current observed after 10 mM-Ba^{2+} is replaced by 10 mM-Ca^{2+}. Current is smallest in mixtures of the two ions. Partial exchange of the more permeant Ba^{2+} for Ca^{2+} paradoxically leads to a decrease in current. This curious 'anomalous mole-fraction behaviour' has previously been observed in post-synaptic anion channels of crayfish muscle (Takeuchi & Takeuchi, 1971), in K^+ channels of starfish eggs (Hagiwara, Miyazaki, Krasne & Ciani, 1977), with the pore-forming antibiotic gramicidin-A (Neher, 1975) and in cardiac Ca^{2+} channels (Hess *et al.* 1983). The effect is often taken as evidence that the channel in question contains two or more binding sites occupied by permeant ions moving in 'single file' (Hille & Schwarz, 1978).

Time course of currents in ion mixtures

Fig. 10*A* shows two superimposed traces of Ca^{2+} inward current recorded during step depolarizations to −10 mV. Besides 10 mM-Ca^{2+}, the external solution contained 108 mM-TMA^+ (light) or a mixture of TMA^+ and Na^+ (heavy trace). During the first second, I_{Ca} is less with Na^+ than without; this was previously attributed to a weak block of Ca^{2+} channels by Na^+. At later times, however, a secondary increase in inward current is seen with Na^+. It is natural to suppose this extra current to be carried by Na^+ through the non-selective permeability mechanism (see also Fig. 1 of Almers *et al.* 1984*a*). This interpretation raises two questions, namely: Why does I_{ns} turn on so slowly and with such a delay? Ordinarily, I_{ns} activates at least as rapidly as I_{Ca} (see Fig. 1). And why does it turn on at all, given the high $[Ca^{2+}]$? These questions may be answered by recalling that both I_{Ca} and I_{ns} are known to flow across the transverse tubular membrane, and that the decline of I_{Ca} signals severe Ca^{2+} depletion from the tubule lumen, especially in the central portion of the tubular system (Almers *et al.* 1981). Only when $[Ca^{2+}]$ in the tubules has fallen to low values does the non-selective conductance become activated. Thus the delayed I_{ns} signals relief from block by Ca^{2+}. During the first second, the channel is selectively permeable to Ca^{2+}, because $[Ca^{2+}]$ in the tubules is high. But when $[Ca^{2+}]$ in the central portion of the tubular system has fallen to low values, the channel there becomes permeable also to monovalent ions such as Na^+.

Fig. 9*B* shows an analogous experiment. Throughout, the external solution contained 10 mM-Ca^{2+} and the impermeant cation TMA^+. The light trace was recorded before, and the heavy trace after addition of 10 mM-Ba^{2+}. Once again, there is at first only little extra current, even though, in the absence of Ca^{2+}, Ba^{2+} is known to be highly permeant. Only later is an extra inward current seen to develop and then decline (see also Fig. 7*D*). As in Fig. 9*A*, we may attribute the secondary inward current to relief of Ca^{2+} channels from block, as a permeant blocking ion becomes depleted from the transverse tubules. Depletion of the blocking ion must precede passage of the second permeant species, as it would otherwise be difficult to explain the biphasic time course in Fig. 9*B*. Since Ca^{2+} blocks I_{Ba} but Ba^{2+} does not block I_{Ca}, Ca^{2+} must be the blocking ion removed from the tubules before Ba^{2+}. Therefore, Fig. 9*B* may be interpreted as follows. When Ca^{2+} is present at sufficient concentration, Ba^{2+} is largely impermeant; this explains why addition of 10 mM-Ba^{2+} causes only little extra current during the first second. As Ca^{2+} inflow causes Ca^{2+} depletion, current first declines. But when $[Ca^{2+}]$ in the tubules has fallen to sufficiently low values, Ca^{2+} channels become fully Ba^{2+}-permeable, and inward current rises for a short while until the tubules become depleted of Ba^{2+} also. Apparently the Ca^{2+} channel selectively extracts Ca^{2+} from the transverse tubular system and only when most of the Ca^{2+} has passed into the myoplasm does the channel become fully Ba^{2+}-permeable. We believe that the delayed current peak in Fig. 7*A* (block of I_{Ba} by 1 mM-Ca^{2+}) and the secondary inward current in Fig. 8*B* (arrow, 5 mM-Ba^{2+} + 5 mM-Ca^{2+}) have a similar explanation. Fig. 9 confirms that when Ca^{2+} and Ba^{2+} are present singly, Ba^{2+} is the more permeant ion (compare currents in Fig. 9*B* and *C*). When both ions are present, however, Ba^{2+} is less permeant than Ca^{2+} since, when given the choice, the channel will pass Ca^{2+} before Ba^{2+} (see Fig. 9*B*).

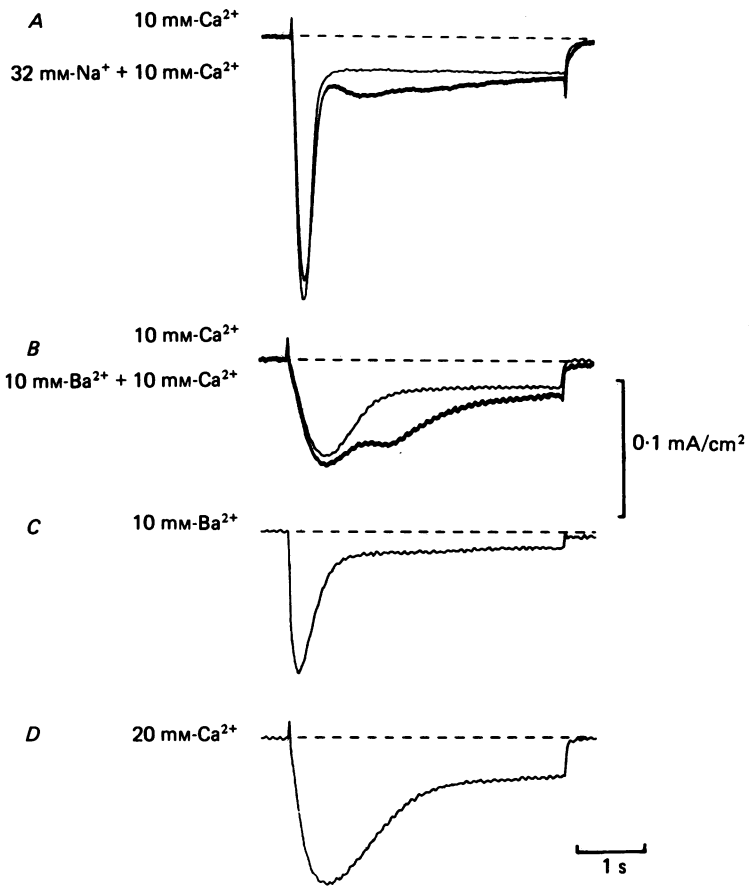

Fig. 9. Interactions between Na^+ and Ca^{2+} (*A*) or Ba^{2+} and Ca^{2+} (*B–D*). Light traces show membrane currents in solutions containing only Ca^{2+} or only Ba^{2+} as permeant cations, while heavy traces were recorded in solutions containing both Ca^{2+} and Na^+ (*A*) or both Ba^{2+} and Ca^{2+} (*B*). The concentrations of Ba^{2+}, Ca^{2+} and Na^+ are indicated in mM. *A*, recorded in Solutions 1 and 5 during step depolarizations from −100 mV to 0 mV. Ends cut in Solution E. Fibre no. 2107, diameter 80 μm, gap 500 μm. *B–D*, recorded during step depolarizations from −80 mV to −10 mV in Solutions 1 and 4 (*B*), Solution 2 (*C*) and Solution 3 (*D*). Ends cut in Solution B with 5 mM-Mg aspartate added. Fibre no. 3067, diameter 80 μm, gap 240 μm.

We have considered whether the secondary inward current in Figs. 9*A* and *B* is due to poor voltage control in the transverse tubular system. In solutions containing only one type of permeant ion, irregular current wave forms are often seen in the 'regenerative' potential range where the peak current–voltage curve has a negative slope. However, such irregularities always disappear under stronger depolarizations to potentials beyond the range of negative slope. The secondary inward currents in the experiments of Fig. 9 were recorded in a region of positive slope conductance and persisted even at positive potentials. Indeed, the delay of the second component increased as peak current diminished at more positive potentials (not shown). This is expected if the second component depends on Ca^{2+} depletion but not if it is due

to uncontrolled depolarization. Also, no second component is apparent in Fig. 9*C* and *D*, even though these traces, recorded at the same potential but with 10 mM-Ba^{2+} only (Fig. 9*C*) or high $[Ca^{2+}]_o$ (Fig. 9*D*), indicated larger currents which should have exacerbated loss of potential control. Throughout our investigation of Ca^{2+} channels in frog muscle, we have observed wave forms as in Fig. 9*A* and *B* only in ion mixtures. Evidently the secondary inward current is related to the simultaneous presence of two types of permeant ions, and not to loss of voltage control.

DISCUSSION

Relationship between non-selective conductance and Ca^{2+} channel

We have previously described a non-selective cation permeability mechanism that is blocked by micromolar external Ca^{2+} concentrations. Since such a mechanism is not expected to operate at physiological external $[Ca^{2+}]$, it is likely that the non-selective conductance is due to one of the known ion channels operating in an abnormal mode. This paper demonstrates that in kinetics and voltage dependence, the non-selective conductance is more similar to the Ca^{2+} channel than to any other known voltage-dependent cation channel. For instance, the tetrodotoxin-sensitive Na^+ channel and the delayed K^+ channel both gate much more rapidly, and another K^+ channel, the inward rectifier, is activated by hyper- rather than depolarization.

Kostyuk & Krishtal (1977) studied an EGTA-induced current in snail neurones which they attributed to modified Ca^{2+} channels and which is similar to current (I_{ns}) through our non-selective conductance. Taken together, the results on snail neurones and frog muscle demonstrate a number of striking similarities between non-selective conductance and Ca^{2+} channels. These similarities are now reviewed.

(*a*) *Where Ca^{2+} channels gate rapidly, non-selective channels are also rapid, while in a tissue with slow Ca^{2+} channels, non-selective channels gate slowly.* At 19–22 °C both EGTA-induced and Ca^{2+} channels in snail neurones open within 10–20 ms at −20 to 0 mV (Kostyuk & Krishtal, 1977). Ca^{2+} channels in frog skeletal muscle open 10 times more slowly, yet the kinetic similarity between I_{Ca} and I_{ns} is preserved (Fig. 1).

(*b*) *Non-selective and Ca^{2+} channels occur at fixed stoicheiometry, which is probably one-to-one.* In frog muscle, the current densities through Ca^{2+} channels and non-selective conductances may vary over a 10-fold range from fibre to fibre, presumably due to a large variation in the number of channels per unit membrane area. Fig. 3 shows that I_{Ca} and I_{ns} are tightly correlated. A related result was reported for *Helix* snail neurones by Krishtal, Pidoplichko & Shakhovalov (1981). They compared I_{Ba} and EGTA-induced currents with the corresponding current fluctuations under conditions where no permeant ions were present intracellularly, and where inward I_{Ba} and EGTA-induced currents depend only weakly on potential. They reported that the ratios of single-channel currents, i_{ns}/i_{Ba}, and of macroscopic currents, I_{ns}/I_{Ba}, were equal to within experimental error. Since I_{Ba} is due to Ca^{2+} channels the result implies that in snail neurones, Ca^{2+} and non-selective channels occur in equal numbers.

(*c*) *Location.* Ca^{2+} channels reside almost exclusively in the transverse tubular system (Nicola Siri, Sánchez & Stefani, 1980; Almers *et al.* 1981) and the same appears

to be true for the non-selective conductance (Takeda, 1977; Potreau & Raymond, 1982). Results suggesting that depletion of Ca^{2+} from the tubules relieves I_{ns} from block (Fig. 9*A* and *B*) also argue in favour of I_{ns} flowing across the tubular membrane.

(*d*) *Pharmacology.* In frog muscle, the Ca^{2+} channel blockers nifedipine and diltiazem block I_{Ca} and I_{ns} channels at identical concentrations (Figs. 4–6). Both currents are also blocked by similar concentrations of well known inorganic Ca^{2+} channel blockers such as Ni^{2+}, Co^{2+} and Cd^{2+} (see later). In snail neurones, both I_{Ca} and I_{ns} are abolished by internal fluoride and by D-600 (Kostyuk & Krishtal, 1977; Kostyuk *et al.* 1983).

The above parallels are most easily explained if the non-selective conductance is due to Ca^{2+} channels. This implies that Ca^{2+} channels undergo a dramatic change in permeability when Ca^{2+} is removed. Almost impermeable to Na^+ at physiological external [Ca^{2+}], they become freely permeable to alkali metal ions when Ca^{2+} is absent. Evidently the physiologically important ability of Ca^{2+} channels to reject monovalent cations depends specifically on the presence of Ca^{2+}: among all the other divalent cations tested (Sr^{2+}, Co^{2+}, Cd^{2+}, Mn^{2+}, Ni^{2+}, Mg^{2+}, Ba^{2+}) Ca^{2+} is the most effective in blocking the non-selective conductance (Almers *et al.* 1984*a*). Interestingly, external Ca^{2+} also diminishes Ba^{2+} permeability (Fig. 7) though this effect requires higher Ca^{2+} concentrations.

Comparison with other tissues

There is evidence that withdrawal of external Ca^{2+} induces a voltage-dependent Na^+ permeability also in preparations other than frog muscle or snail neurones. In cardiac muscle (Rougier, Vassort, Garnier, Gargouil & Coraboeuf, 1969), in gastrointestinal smooth muscles of various vertebrates (Prosser, Kreulen, Weigel & Yau, 1977), in striated muscle of insect larvae (Yamamoto & Washio, 1979), and in mouse oocytes (Yoshida, 1983), slow action potentials are observed when external [Ca^{2+}] is lowered to submicromolar levels by Ca^{2+} chelators such as EDTA or EGTA. These action potentials are tetrodotoxin-resistant, but are abolished when external Na^+ is replaced by large organic cations such as choline (frog heart) or Tris (smooth and insect larval muscle). They are also abolished by substances known to block Ca^{2+} channels, such as Co^{2+}, Mn^{2+} and D-600. Throughout, this Na^+ permeability was attributed to Ca^{2+} channels. Evidently, I_{ns} through Ca^{2+} channels at low $[Ca^{2+}]_o$ is found not only in different tissues (neurones, oocytes, smooth, cardiac and skeletal muscle) but also in different phyla, such as molluscs, arthropods and vertebrates. Hence I_{ns} reflects a general property of Ca^{2+} channels.

Since I_{ns} at -20 mV is half-blocked by only 0·7 μM-Ca^{2+} in frog muscle (Almers *et al.* 1984*a*) and 0·3 μM in snail neurones (Kostyuk *et al.* 1983), Ca^{2+} must bind to Ca^{2+} channels with high affinity. The need for Ca^{2+} chelators in recording I_{ns} from smooth and cardiac muscle confirms this view also for other tissues. There is no direct evidence on how Ca^{2+} inhibits the passage of monovalent cations through Ca^{2+} channels. It has been suggested that Ca^{2+} binding to an extracellular control site causes a structural change in the channel's selectivity filter (Kostyuk *et al.* 1983). Ca^{2+}-induced structural changes are well established for at least two intracellular regulatory proteins, troponin and calmodulin.

However, an *extracellular* site with micromolar dissociation constant for Ca^{2+} is

unlikely to form part of any physiological control mechanism, as such a site would always be filled at the millimolar $[Ca^{2+}]_o$ present physiologically. One also wonders why there should be a universal need for Ca^{2+} channels to be capable of changing their permeability to Na^+ and K^+. It is attractive to suppose instead that block of I_{ns} and I_{Ba} by Ca^{2+} reflects some feature of the mechanism of ion permeation through Ca^{2+} channels. In particular, we propose that Ca^{2+} channels, being innately permeable to all physiological inorganic cations, derive their Ca^{2+} selectivity from high-affinity Ca^{2+}-binding sites located within the aqueous pore, and that these sites represent normal way stations for Ca^{2+} during permeation. Below, this hypothesis is explored quantitatively.

A model for ion permeation through Ca^{2+} channels

In this theoretical section we demonstrate that the transition of Ca^{2+} channels from their usual Na^+-rejecting form to a Na^+-permeable state does not require a change in channel structure. Instead, this effect as well as the observed change in I_{Ba} are predictable consequences of Ca^{2+} dissociating from binding sites within the pore.

The data we wish to account for are shown in Figs. 8 and 11*A*. In Fig. 11*A* (data from Almers *et al.* 1984*a*), membrane current at a fixed potential (−20 to 0 mV) has been plotted against external pCa. At pCa > 5 current is carried mainly by Na^+, as it is abolished when TMA^+ replaces Na^+. Half-blockage of this current occurs at 0·7 μM, and this is assumed to be the concentration required to load the highest-affinity Ca^{2+} binding site within the pore. At pCa < 4 current is carried by Ca^{2+}. Because current increases with increasing $[Ca^{2+}]_o$ over the range 1–10 mM and beyond (Almers & Palade, 1981), we must assume that the pore can bind at least one more Ca^{2+} ion at lower affinity. The existence of at least two sites that may be simultaneously occupied by divalent cations is also suggested by the anomalous mole-fraction behaviour in Fig. 8, and by the fact that the permeant Ca^{2+} blocks Ba^{2+} currents.

Fig. 10*A* illustrates our view of the Ca^{2+} channel as an aqueous pore with two ion binding sites. The distance between them may be as in a troponin-C molecule, whose Ca^{2+}-binding sites are thought to be spaced 1·15 nm apart (Kretsinger & Barry, 1975). Though both sites may be occupied simultaneously by one ion each, we assume that while an ion is bound to one of the sites, no other ion may pass. Na^+ and Ba^{2+} are less tightly bound than Ca^{2+}; this feature makes the pore Ca^{2+} selective in the sense that it will pass Ca^{2+} in preference to Ba^{2+} or Na^+ in ion mixtures (see, for example, Fig. 9 and accompanying discussion). We view Fig. 10*A* as a minimal model and have included neither the binding sites for Ca^{2+} channel blockers (see later), nor the gating machinery, nor the surface charges likely to be present.

Rate-theory description of ion transport. This approach to ion channels is now well established, and the extensive literature on the subject has been reviewed by Hille & Schwarz (1978). Our model is a slightly modified version of one proposed by Begenisich & Cahalan (1980) for Na^+ channels of squid axons. Fig. 10*B* is intended to be a translation of Fig. 10*A* into the terminology of rate theory. It plots, against position along an empty pore, the potential energy of a Ca^{2+} (continuous curve) or Na^+ (dashed curve) with respect to bulk solution and when there is no membrane potential. For simplicity, the pore is assumed to be symmetric, with two energy minima representing two identical ion binding sites with high affinity for Ca^{2+} and

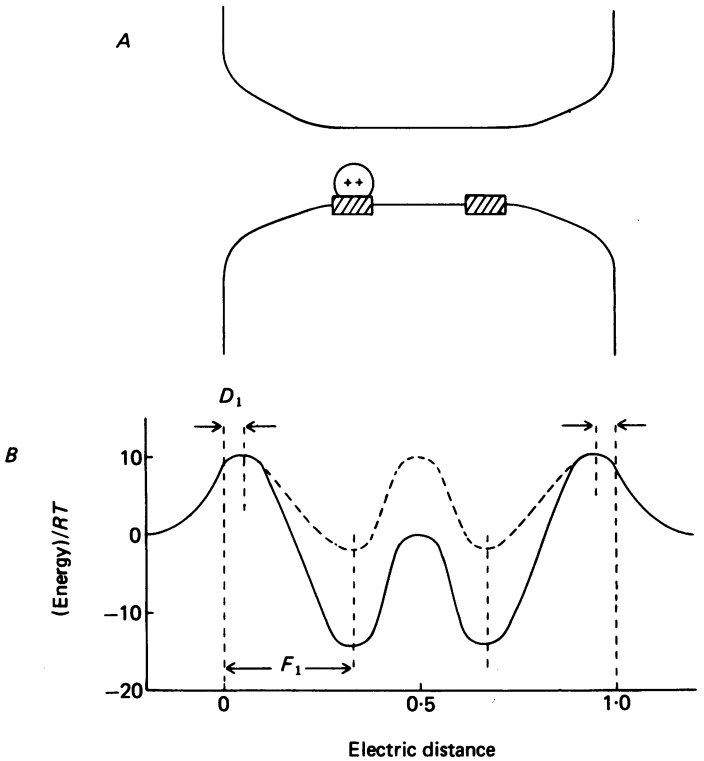

Fig. 10. *A*, schematic drawing of Ca^{2+} channel with two binding sites (hatched), one of them complexed with a divalent cation. *B*, energy profile of the Ca^{2+} channel. The ordinate plots energy (in J/mol) divided by *RT* for an empty pore at zero membrane potential; the abscissa gives the fraction of the transmembrane potential experienced at any given point ('electric distance', see text). The energy profiles are symmetric about the mid line (abscissa 0·5), with $D_1 = 0{\cdot}05$ and $F_1 = 0{\cdot}33$. Profiles shown are for Ca^{2+} (continuous curve) and Na^+ (dashed curve).

a lower one for Na^+. The energy of Ca^{2+} bound to one of the sites in an otherwise empty pore is given by

$$\Delta G_w = RT \ln K_D, \tag{1}$$

where *R* and *T* are gas constant and absolute temperature, and where K_D is the dissociation constant for Ca^{2+}. As a first approximation, K_D is given by the $[Ca^{2+}]$ required to reduce I_{ns} 2-fold, namely 0·7 μM.

The rates of arrival and departure of ions in the sites are assumed to be exponential functions of the energy maxima (energy barriers) over which the ions must pass. To illustrate a particularly simple case, consider the rate constant $k_{1,2}$ for entry of extracellular Ca^{2+} into the outer site of an empty pore at zero membrane potential:

$$k_{1,2} = [Ca^{2+}]_o \nu \exp(-\Delta G_e/RT), \tag{2}$$

where ν is a constant multiplier of all rate constants and ΔG_e is the height of the outer energy barrier with respect to bulk fluid. The physical significance of the outer barriers

is discussed later. Besides depending on extra- or intracellular ion concentrations, rate constants also depend on the probability of finding a Na^+, Ba^{2+}, or Ca^{2+} in a given site, and on what ion, if any, occupies the neighbouring site. For example, the rate at which Ca^{2+} ions go from the outer site into the external solution is given by

$$k_{2,1} = A\nu \exp\left[-(\Delta G_e - \Delta G_w)/RT\right] \tag{3}$$

for zero membrane potential and if no other ion is in the pore. The factor A is proportional to the number of outer sites being occupied by a Ca^{2+} ion, and depends on the various other rate constants in the model as well as the internal ion concentrations. When two species of permeant ions are present on both sides of the membrane, the model contains twenty-eight rate constants determined by ten independent parameters.

The effect of membrane potential is included by assuming either that potential varies linearly with distance, or that the abscissa corresponds to an 'electrical distance', that is, to the fraction of the transmembrane potential drop experienced at any given point. With a transmembrane potential E, we have

$$k_{1,2} = [Ca^{2+}]_o \nu \exp\left[-(\Delta G_e + FEzD_1)/RT\right] \tag{4}$$

and

$$k_{2,1} = A\nu \exp\left[-(\Delta G_e - \Delta G_w - FEz(F_1 - D_1))/RT\right], \tag{5}$$

where F is Faraday's constant, z the valency of the ion in question, and D_1, F_1 are the electric distances of the outer barrier and outer site, respectively. Equations (2)–(5) are for illustration only; details can be found in the papers by Hille & Schwarz (1978) and Begenisich & Cahalan (1980).

Ion repulsion. Having high-affinity Ca^{2+}-binding sites in the pore puts constraints on explaining the high Ca^{2+} fluxes observed in other preparations by single-channel recording or noise analysis. To illustrate this, consider a soluble Ca^{2+} receptor in bulk fluid

$$Ca^{2+} + R \underset{k_2}{\overset{k_1}{\rightleftharpoons}} Ca\text{–}R$$

with dissociation constant $K_D = k_2/k_1$. If the forward rate constant is diffusion-limited, and the receptor is a circular target of radius a (in cm), then the rate at which ions arrive at the target is k_1 $[Ca^{2+}]$ where k_1 can be calculated by (e.g. see Hille, 1984):

$$k_1 = 2\pi a D_{Ca} N \times 10^{-3}, \tag{6}$$

where N is Avogadro's constant and D_{Ca} is the diffusion coefficient for Ca^{2+}, namely 8×10^{-6} cm^2/s (Wang, 1953). Assuming $a = 0{\cdot}3$ nm, k_1 becomes 10^9/ms. This, incidentally, would correspond to an energy barrier of 8·7 RT at 20 °C in eqns. (2)–(5) if one assumes $\nu = kT/h$ where k and h are Boltzmann's and Planck's constants, respectively. With $k_2 = k_1 K_D$ being the rate constant for dissociation of the Ca–R complex, the maximum rate at which ions could leave one receptor is 700/s for $K_D = 0{\cdot}7 \times 10^{-6}$ M. Observed single-channel fluxes are much higher. For instance, Fenwick, Marty & Neher (1982) observed 0·09 pA or 280000 Ca^{2+} ions/ s in single Ca^{2+} channels of chromaffin cells. The difficulty of reconciling high fluxes with high-affinity sites in pores was also recognized by Kostyuk, Mironov & Doroshenko (1982).

The problem disappears if we consider that when a first site in the pore is occupied, the affinity of the second site is likely to be reduced due to ion repulsion. Ion repulsion is expected, since the binding sites in the pore are surrounded by a medium of relatively low dielectric constant (i.e. the membrane). The energy of repulsion per mole of ion pairs in an infinite homogenous medium is given by

$$\Delta G = \frac{Ne^2}{4\pi\epsilon\epsilon_0}\frac{z_1 z_2}{r}, \tag{7}$$

where N is Avogadro's constant, e the elementary charge, ϵ_0 and ϵ are the dielectric constants of vacuum and the surrounding medium, respectively, z_1 and z_2 are the valencies and r the distance between the two ions. Since the pore is not an infinite homogenous medium, a more explicit calculation along the lines given by Levitt (1978) would be preferable. Nevertheless, eqn. (7) illustrates that the energies of repulsion may be large. For two Ca^{2+}-occupied sites rigidly separated by 1·15 nm, repulsion will diminish the probability of simultaneous occupancy by 12 when $\epsilon = 80$ as in water, and by 12^4 or 20000 when $\epsilon = 20$, as may be the case inside an ion channel. Repulsion is steeply dependent on the valency of the repelling ions. If the probability of simultaneous occupancy by two monovalent ions is reduced by a factor Q, this probability is reduced Q^4-fold for two divalent ions.

We assume that the only effect of ion repulsion is to increase the rate constants for ions leaving a doubly occupied pore. These rate constants are increased by a factor Q if both ions in the pore are monovalent, Q^4 if both are divalent, and Q^2 if they are of mixed valency. Besides increasing departure rates from a doubly-occupied pore, ion repulsion also ensures that the vacant site in a singly occupied pore has a low affinity and explains why Ca^{2+} influx increases with external $[Ca^{2+}]$ even at high concentrations.

Choice and physical significance of parameters. Among all parameters, the depth of the energy well for Ca^{2+}, ΔG_w, is perhaps the one that is most directly determined in our measurements. By eqn. (1), $\Delta G_w = -14{\cdot}2\,RT$ would correspond to $K_D = 0{\cdot}7\ \mu M$, so a closely similar value, $-14{\cdot}5\,RT$, was chosen for the site in equilibrium with the external fluid. The same value was chosen also for the other site, even though future studies of the effect of internal $[Ca^{2+}]$ may indicate otherwise. Kostyuk *et al.*'s (1983) result on snail neurones suggests that K_D for Ba^{2+} is 70 times larger than for Ca^{2+}, so we set $\Delta G_w = -10{\cdot}3\,RT$ for Ba^{2+}. The wells for Na^+ were set at $-2\,RT$, corresponding to $K_D = 140$ mM by eqn. (1).

The outer energy barriers are assumed to symbolize mainly the diffusional access and departure of ions to and from the pore, and their height (10·3 RT for Ca^{2+}, 9·15 RT for Ba^{2+} and 10·0 RT for Na^+) is only slightly above the minimum prescribed by the diffusion limit (8·7 RT for Ca^{2+} and 8·2 RT for Na^+). Realistically, they should also include a contribution from any dehydration that may be required before an ion can bind. The membrane potential is assumed to have only a small influence on diffusional access, so these energy barriers are drawn at negligible electric distance from the inner and outer mouths. Also, Levitt (1978) has calculated that an ion at the extreme end (or outside) of an aqueous pore experiences little repulsion by an ion already present at the other end of the pore, therefore it seems reasonable to have ion repulsion influence only the departure from sites, and not the arrival. Put another way, electrostatic repulsion from an ion deep in the pore is unlikely to have significant effect

on diffusional access from bulk medium, which is assumed here to make the main contribution to the outer barriers. The position of the wells and the height of the central barriers were chosen arbitrarily. The only significant effect of making the central barrier for Na^+ the same as for Ca^{2+} would be to increase by 50% the maximum I_{ns} reached asymptotically at high pCa.

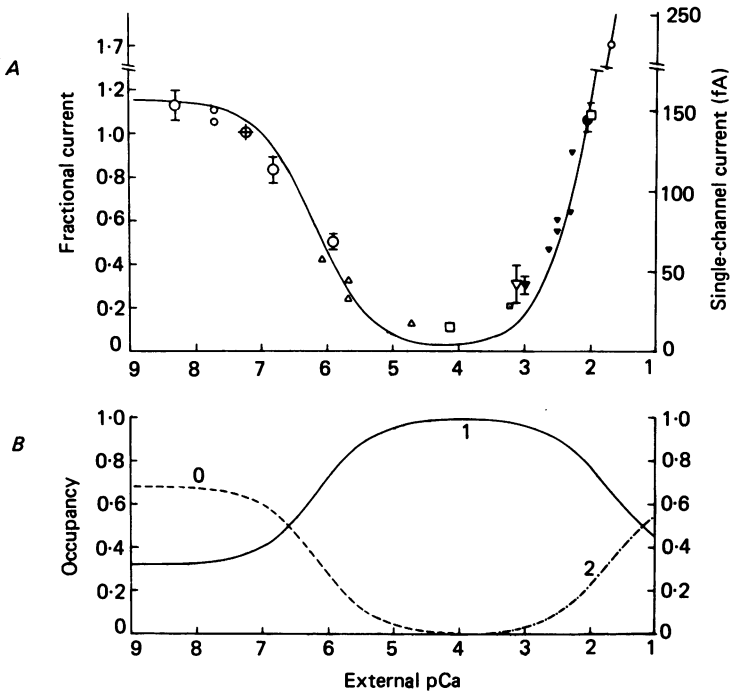

Fig. 11. *A*, peak inward current plotted as a function of pCa ($= -\log [Ca^{2+}]_o$). Data are those of Almers, McCleskey & Palade (1984*a*) except for a single measurement (rightmost), which was obtained from an experiment as in Fig. 9. The curve was calculated as described in the text, using $\nu = kT/h$ and a modified version of a computer program kindly provided by Dr Ted Begenisich. Parameters used for Ca^{2+} were: $[Ca^{2+}]_i = 0$, height of outer barriers 10·3 *RT*, central barrier, 0, depths of wells −14·5 *RT*. Parameters used for Na^+ were: $[Na^+]_i = [Na^+]_o = 32$ mM, all barriers 10·0 *RT*, all wells −2·0 *RT*. Membrane potential of −20 mV was assumed throughout. Ion repulsion factor was 11·89; with this value, the probability of two Ca^{2+} ions occupying the pore simultaneously is $(11{\cdot}89)^4 = 20000$-fold lower than without repulsion. *B*, fraction of pores occupied by no (dashed curve), one (continuous curve), or two (dashes and dots) ions. Except at the lowest $[Ca^{2+}]_o$, the pore is occupied exclusively by Ca^{2+}.

We have explored whether high fluxes through pores with high-affinity sites can be achieved by means other than ion repulsion. To a degree, this is possible by raising the internal (but not the external) energy well to about −9 *RT*. To increase flux it is then also necessary to lower the Ca^{2+} entry barriers to 6 *RT*. This model shows considerably more severe inward rectification than is observed experimentally (Fenwick *et al.* 1982).

Comparison with data. The continuous curve in Fig. 11*A* was calculated with the

energy profiles of Fig. 10*B* and with an ion repulsion factor of $Q = 11{\cdot}89$. It was assumed that there is no internal Ca^{2+}, and that Cs^+ and Na^+ behave identically in the pore, so that the reversal potential at high external pCa is 0 mV. The calculation reproduces our experimental results well. Half-blockage of I_{ns} occurs at submicromolar $[Ca^{2+}]$, and above $\sim 0{\cdot}1$ mM concentration, Ca^{2+} becomes a current carrier and I_{Ca} grows with $[Ca^{2+}]_o$. At 100 mM, I_{Ca} is calculated to be three times larger than at 10 mM (not shown); changing $[Ca^{2+}]_o$ from 10 to 100 mM increased I_{Ca} 3·5-fold (Almers *et al.* 1984*a*). The single-channel current at 5 mM-$[Ca^{2+}]_o$ is 0·09 pA, as obtained by Fenwick *et al.* (1982) at -12 mV in chromaffin cells. The reversal potential E_{rev} at 10 mM-external $[Ca^{2+}]$ and 32 mM-internal Na^+ is $+169$ mV; under more physiological conditions, that is, with $[Ca^{2+}]_o = 1{\cdot}8$ mM and 140 mM internal monovalent cation, $E_{rev} = 76$ mV.

To illustrate the mechanism of ion permeation, Fig. 11*B* shows the calculated occupancies as a function of external pCa. Since Na^+ does not bind very tightly, about 70 % of the pores at high pCa are unoccupied. As $[Ca^{2+}]_o$ is increased, Ca^{2+} occupies vacant pores as well as displacing Na^+. The disappearance of unoccupied pores coincides with block of I_{ns}. At still higher $[Ca^{2+}]_o$, all pores are occupied by at least one Ca^{2+} and Ca^{2+} becomes a current carrier. When an external Ca^{2+} manages to bind to a vacant external site, it can push the resident Ca^{2+} off the internal site and into the myoplasm, thereby generating I_{Ca}. The frequency with which this happens (and therefore I_{Ca}) grows with external Ca^{2+} until, at molar $[Ca^{2+}]_o$, both sites become almost permanently occupied and flux at a fixed potential reaches a limiting value determined by the rate at which Ca^{2+} can leave the internal site in the presence of ion repulsion.

Assuming physiological concentrations of 125 mM for external and 140 mM for internal monovalent cations, further model calculations (not shown) gave the following results. In the absence of Ca^{2+}, the *current–voltage curve* of open Ca^{2+} channels is approximately linear between -100 and $+100$ mV. With 1 mM-external and no internal Ca^{2+}, the current–voltage curve is qualitatively similar to that recorded by Fenwick *et al.* (1982). Ca^{2+} channel conductance is relatively large at negative potentials, becomes small near the reversal potential (55 mV) and increases again at more positive potentials as the channel becomes increasingly permeable to monovalent cations. For I_{ns}, the model predicts a complex *voltage dependence of block by* Ca^{2+}. At fixed external Ca^{2+} (e.g. 1 μM), block is strongest at slightly negative potentials, and becomes weaker at more extreme potentials of either sign. Such a voltage dependence was seen for block of Na^+ channels by H^+ (Begenisich & Danko, 1983). In our calculation, the predicted voltage dependence over the range -100 to 20 mV is so slight as to be difficult to detect experimentally, and was, in fact, not detected in Kostyuk *et al.*'s (1983) work on snail neurones. Only at strongly positive potentials (> 50 mV) is there a pronounced relief from block. With Ba^{2+}, the model predicts an *anomalous mole fraction behaviour* that is qualitatively similar to that observed with Ca^{2+}/Ba^{2+} mixtures (continuous line in Fig. 8). Hess & Tsien (1984) have successfully applied a model similar to Fig. 10 to cardiac Ca^{2+} channels, and have reached similar conclusions regarding the mechanism of ion permeation and selectivity.

Inorganic Ca^{2+} *channel blockers.* A number of impermeant or sparingly permeant

ions such as Co^{2+}, Cd^{2+}, Ni^{2+} and Mn^{2+} are well known to block I_{Ca} at millimolar concentrations. Since in our model permeation and block in ion mixtures are attributed to competition for two sites with much higher affinity to Ca^{2+} than to Na^+ one expects that the inorganic blockers should be vastly more effective in blocking I_{ns} than I_{Ca}. Instead, they block both currents approximately equally. At 10 mM-Ca^{2+}, for example, I_{Ca} is half-blocked by about 1 mM-Ni^{2+}, 1 mM-Co^{2+} and 0·4 mM-Cd^{2+} (Almers, McCleskey & Palade, 1984*b*), and similar concentrations are required to block I_{ns} (Almers *et al.* 1984*a*). Failure of these foreign divalent cations to block I_{Na} at the appropriate low concentrations indicates that they cannot compete for the sites in Fig. 10. The finding could be explained if, in addition to the high-affinity Ca^{2+} sites in the pore, the external face of the channel bears a site of lower affinity for which divalent cations may compete. Evidence for such a site is reviewed by Hagiwara (1975).

The selectivity of Ca^{2+} channels

Previous work has attributed the selectivity of monovalent cation channels entirely to molecular sieving, that is, to the rejection of impermeant ions by high energy barriers (Bezanilla & Armstrong, 1972; Hille, 1975). Indeed, Bezanilla & Armstrong (1972) have shown theoretically that in pores occupied by at most one ion, *selectivity by rejection* of impermeants is the only conceivable mechanism. Our work demonstrates that (a) the well known ability of Ca^{2+} channels to exclude monovalent cations shows itself only in the presence of Ca^{2+}, and (b) that the well known high permeability to Ba^{2+} is seen only in the absence of Ca^{2+}. Evidently the selective permeability of Ca^{2+} channels depends on Ca^{2+}, and expresses itself only when Ca^{2+} is bound to a high-affinity site. We have proposed that the site resides within the aqueous pore, and that its specific affinity for Ca^{2+} forms the basis for the physiologically important selectivity of Ca^{2+} channels for Ca^{2+} over the majority ions Na^+ and K^+. Hence in Ca^{2+} channels we have *selectivity by affinity* for Ca^{2+}. In our model, we require at least two binding sites, and explain the experimentally observed high single-channel fluxes by electrostatic repulsion between ions bound to the two sites. Electrostatic repulsion is expected to be much larger between divalent than between monovalent ions, so it is understandable why selection by affinity may play a larger role in channels selective for multivalent ions.

While the selection of Ca^{2+} over Na^+, K^+ and Ba^{2+} may be attributed to affinity for Ca^{2+}, the exclusion of the large organic cations TMA^+ and TEA^+ probably occurs by sieving, i.e. by rejection. Mg^{2+} is another ion that is probably selected against by rejection since it blocks I_{ns} only at high concentrations (Almers *et al.* 1984*a*) and yet carries only small currents through Ca^{2+} channels even when Ca^{2+} is absent (Almers & Palade, 1981). Evidently selection by affinity and by rejection may occur side-by-side.

While the Ca^{2+} channel is probably the most striking example for selection by affinity, it may not be the only one. For instance, the 'selectivity' of the gramicidin channel for Tl^+ over Na^+ (see Neher, 1975; Urban, Hladky & Haydon, 1978; Eisenmann, Enos, Hagglund & Sandblom, 1980) has previously been treated with theories similar to the one used here, and may be viewed as being due to a higher affinity for Tl^+. Also, K^+ channels have long been recognized to be single-file pores

(for review see Hille & Schwarz, 1978) and it is conceivable that their remarkable selectivity for K^+ owes much to selective binding of K^+ to sites in the channel. In summary, the study of Ca^{2+} channels has added a feature to our understanding of selectivity among small cations. Selective binding of ions in single-file pores could be a general way to achieve high ion selectivity while retaining high single-channel fluxes. That selectivity by affinity is compatible with high single-channel fluxes seems to answer an important argument against Eisenmann's (1962) theory of selectivity.

This work owes much to discussions with Dr Bertil Hille. Our thanks are due to Dr Philip T. Palade for participating in early experiments related to this work, to Drs Hille, Palade and Peter B. Detwiler for their comments on the manuscript, to Dr Ted Begenisich at the University of Rochester for his computer program for calculating ion fluxes in single-file pores, to Dr Richard W. Tsien for participating in an exchange of manuscripts, and to Lea Miller for her expert help in preparing this manuscript. Supported by USPHS grant AM-17803.

REFERENCES

ALMERS, W., FINK, R. & PALADE, P. T. (1981). Calcium depletion in frog muscle tubules: the decline of calcium current under maintained depolarization. *J. Physiol.* **312**, 177–207.

ALMERS, W., MCCLESKEY, E. W. & PALADE, P. T. (1982). Frog muscle membrane: a cation-permeable channel blocked by micromolar external [Ca^{2+}]. *J. Physiol.* **332**, 52–53*P*.

ALMERS, W., MCCLESKEY, E. W. & PALADE, P. T. (1984*a*). A non-selective cation conductance in frog muscle membrane blocked by micromolar external calcium ions. *J. Physiol.* **353**, 565–583.

ALMERS, W., MCCLESKEY, E. W. & PALADE, P. T. (1984*b*). Ca channels in vertebrate skeletal muscle. In *Calcium and Skeletal Muscle Contractility*. New York: Plenum Press (in the Press).

ALMERS, W. & PALADE, P. T. (1981). Slow calcium and potassium currents across frog muscle membrane: measurements with a vaseline-gap technique. *J. Physiol.* **312**, 159–176.

BEGENISICH, T. & CAHALAN, M. D. (1980). Sodium channel permeation in squid axons. I. Reversal potential experiments. *J. Physiol.* **307**, 217–242.

BEGENISICH, T. & DANKO, M. (1983). Hydrogen block of the sodium pore in squid axons. *J. gen. Physiol.* **82**, 599–618.

BEZANILLA, F. & ARMSTRONG, C. M. (1972). Negative conductance caused by entry of sodium and cesium ions into the potassium channels of squid giant axons. *J. gen. Physiol.* **60**, 588–608.

EISENMANN, G. (1962). Cation selective glass electrodes and their mode of operation. *Biophys. J.* **2**, 259–323.

EISENMANN, G., ENOS, B., HAGGLUND, J. & SANDBLOM, J. (1980). Gramicidin as an example of a single-filing ion channel. *Ann. N.Y. Acad. Sci.* **339**, 8–21.

FENWICK, E. M., MARTY, A. & NEHER, E. (1982). Sodium and calcium channels in bovine chromaffin cells. *J. Physiol.* **331**, 599–635.

FOSSET, M., JAIMOVICH, E., DELPONT, E. & LAZDUNSKI, M. (1983). [^{3}H]Nitrendipine receptors in skeletal muscle. *J. biol. Chem.* **258**, 6086–6092.

HAGIWARA, S. (1975). Ca-dependent action potential. In *Membranes: a Series of Advances*, vol. 3, ed. EISENMANN, G. New York: Marcel Dekker.

HAGIWARA, S., MIYAZAKI, S., KRASNE, A. & CIANI, S. (1977). Anomalous permeabilities of the egg cell membrane of a starfish in K^+–Tl^+ mixtures. *J. gen. Physiol.* **70**, 269–281.

HAGIWARA, S. & OHMORI, H. (1982). Studies of calcium channels in rat clonal pituitary cells with patch electrode voltage clamp. *J. Physiol.* **331**, 231–252.

HESS, P., LEE, K. S. & TSIEN, R. W. (1983). Ion–ion interactions in the Ca^{2+} channel of single heart cells. *Biophys. J.* **41**, 293a.

HESS, P. & TSIEN, R. W. (1984). Mechanism of ion permeation through calcium channels. *Nature, Lond.* (in the Press).

HILLE, B. (1975). Ionic selectivity of Na and K channels of nerve membranes. In *Membranes: a Series of Advances*, vol. 3, ed. EISENMANN, G. New York: Marcel Dekker.

HILLE, B. (1984). *Ionic Channels of Excitable Membranes*. Sunderland, MA: Sinauer Associates.

HILLE, B. & CAMPBELL, D. T. (1976). An improved vaseline gap voltage clamp for skeletal muscle fibres. *J. gen. Physiol.* **67**, 265–293.

HILLE, B. & SCHWARZ, W. (1978). Potassium channels as multi-ion, single-file pores. *J. gen. Physiol.* **72**, 409–442.

HODGKIN, A. L. & NAKAJIMA, S. (1972). Analysis of the membrane capacity in frog muscle. *J. Physiol.* **221**, 121–136.

KOSTYUK, P. G. & KRISHTAL, O. A. (1977). Effects of calcium and calcium-chelating agents on the inward and outward current in the membrane of mollusc neurones. *J. Physiol.* **270**, 569–580.

KOSTYUK, P. G., MIRONOV, S. L. & DOROSHENKO, P. A. (1982). Energy profile of the calcium channel in the membrane of mollusc neurones. *J. Membrane Biol.* **70**, 181–189.

KOSTYUK, P. G., MIRONOV, S. L. & SHUBA, YA. M. (1983). Two ion-selecting filters in the calcium channel of the somatic membrane of mollusc neurons. *J. Membrane Biol.* **76**, 83–93.

KRETSINGER, R. H. & BARRY, C. D. (1975). The predicted structure of the calcium-binding component of troponin. *Biochim. biophys. Acta* **405**, 40–52.

KRISHTAL, O. A., PIDOPLICHKO, V. I. & SHAKHOVALOV, Y. A. (1981). Conductance of the calcium channel in the membrane of snail neurones. *J. Physiol.* **310**, 423–434.

LEE, K. S. & TSIEN, R. W. (1983). Mechanism of calcium channel blockade by verapamil, D-600, diltiazem, and nitrendipine in single dialysed heart cells. *Nature, Lond.* **302**, 790–794.

LEVITT, D. G. (1978). Electrostatic calculations for an ion channel. I. Energy and potential profiles and interactions between ions. *Biophys. J.* **22**, 209–219.

NEHER, E. (1975). Ionic specificity of the gramicidin channel and the thallous ion. *Biochim. biophys. Acta* **401**, 540–544.

NICOLA SIRI, L., SÁNCHEZ, J. A. & STEFANI, E. (1980). Effect of glycerol treatment on the calcium current of the frog skeletal muscle. *J. Physiol.* **305**, 87–96.

POTREAU, D. & RAYMOND, G. (1982). Existence of a sodium-induced calcium release mechanism on frog skeletal muscle fibres. *J. Physiol.* **333**, 463–480.

PROSSER, C. L., KREULEN, D. L., WEIGEL, R. J. & YAU, W. (1977). Prolonged action potentials in gastrointestinal muscles induced by calcium chelation. *Am. J. Physiol.* **233**, C19–24.

REUTER, H. & SCHOLZ, H. (1977). A study of the ion selectivity and the kinetic properties of the calcium-dependent slow inward current in mammalian cardiac muscle. *J. Physiol.* **264**, 17–47.

ROUGIER, O., VASSORT, G., GARNIER, D., GARGOUIL, Y. M. & CORABOEUF, E. (1969). Existence and role of a slow inward current during the frog atrial action potential. *Pflügers Arch.* **308**, 91–110.

TAKEDA, K. (1977). Prolonged sarcotubular regenerative response in frog sartorius muscle. *Jap. J. Physiol.* **27**, 379–389.

TAKEUCHI, A. & TAKEUCHI, N. (1971). Anion interaction at the inhibitory post-synaptic membrane of the crayfish neuromuscular junction. *J. Physiol.* **212**, 337–351.

URBAN, B. W., HLADKY, S. B. & HAYDON, D. A. (1978). The kinetics of ion movement in the gramicidin channel. *Fedn Proc.* **37**, 2628–2632.

WANG, J. H. (1953). Tracer diffusion in liquids. IV. Self-diffusion of calcium ion and chloride ion in aqueous calcium chloride solutions. *J. Am. chem. Soc.* **75**, 1769–1770.

YAMAMOTO, D. & WASHIO, H. (1979). Permeation of sodium through calcium channels of an insect muscle membrane. *Can. J. Physiol. Pharmacol.* **57**, 220–223.

YOSHIDA, S. (1983). Permeation of divalent and monovalent cations through the ovarian oocyte membrane of the mouse. *J. Physiol.* **339**, 631–642.